Int. J. Heat Mass Transfer. Vol. 33, No. 7, pp. 1511–1520, 1990
Printed in Great Britain

0017-9310/90 $3.00+0.00

Radiation induced ignition of solid fuels

S. H. PARK and C. L. TIEN
Department of Mechanical Engineering, University of California, Irvine, CA 92717, U.S.A.

(*Received* 7 *June* 1989 *and in final form* 5 *October* 1989)

Abstract—The present work reports that gas-phase radiation absorption is one of the critical mechanisms responsible for the gas-phase ignition of solid fuels which are exposed to a strong external thermal radiation. A one-dimensional transient model includes the effects of the gas-phase absorption of incident thermal radiation; in-depth absorption by the solid phase; and natural convection along the fuel surfaces. A numerical simulation confirms that the decomposition products significantly attenuate the incident radiation, which has been already observed experimentally. In spite of natural convection flows which dilute the absorbing gases and increase heat losses, absorbed radiant energy plays an important role in the induction of the gas-phase thermal runaway. Thus, ignitable domains are considerably different from those obtained without considerations of the gas-phase radiation absorption.

INTRODUCTION

RADIATIVE ignition of solid fuels represents the integration of complicated interactions of heat and mass transfer and chemical reactions. In spite of such complexities, the present study attempts to analyze the phenomena systematically using a simplified model in order to understand the fundamental mechanisms in radiative ignition of solid fuels. Especially, the role of gas-phase radiation absorption during ignition processes.

Studies on ignition of solid fuels have been concerned with their ignitability and ignition mechanisms. Ignitability is a critical factor both in the selection of construction materials to prevent unwanted ignition accidents and in the grading and selection of solid propellants. Ignitability can be described by the ignitable domain map [1] which shows the range of thermophysical and chemical properties of fuels and the ambient conditions for which ignition can occur. Ignition mechanisms need to be understood to explain experimentally observed ignition behavior and to predict the phenomenon in advance.

A parametric study conducted by Kashiwagi [1] on radiation induced ignition of a solid fuel demonstrated that gas-phase reaction must be included in order to understand the radiative ignition of a solid fuel and to find its ignitable domain. Kindelan and Williams [2–4] explored gas-phase ignition in the radiative ignition process using an asymptotic method and defined three sequential ignition processes: initial inert heating, short transition, and long transport-controlled stages. Kumar [5] carried out two-dimensional analysis of the radiative ignition of a composite solid propellant to include its inhomogeneity. Effects of a natural convection boundary layer along a vertical surface were included in the integral formulation by Gandi and Kanury [6]. Kashiwagi [1] showed that effects of the in-depth absorption of the incident radiation by the solid fuel are significant on the ignition delay time. Mutoh *et al.* [7] conducted an experimental study to explore the radiation induced ignition behavior of PMMA by examining the temperature and concentration fields in the plume formed over the fuel surface. During the ignition process, attenuation of the incident radiation by decomposition products in the gas phase was observed experimentally by Kashiwagi [8, 9]. He postulated that under auto-ignition conditions, the solid (PMMA) could be ignited due to the absorption of the incident radiation by decomposition products in the gas phase. Recently, Amos and co-workers [10, 11] investigated the role of radiation absorption in the induction of gas-phase ignition at zero gravity and subsequent flame propagation.

A significant participation of pyrolyzed gases evolved during the ignition process in radiative energy exchanges has been recognized by the previously stated experimental and theoretical studies. However, the importance of gas-phase absorption of radiation energy in the gas-phase ignition process has been questioned [12], probably because of the dilution and flushing of absorbing gases by gravity induced flows. Therefore, the main objective of the present study is to theoretically investigate the radiative ignition phenomena using a simplified model and to clarify the role of gas-phase absorption of incident radiation during the ignition process under the normal gravitational conditions. A one-dimensional transient model developed here includes not only the enhancement effects of the interaction between pyrolyzed absorbing gases and the incident radiation, but also the retardation effects of natural convection on the ignition behavior of solid fuels.

ANALYSIS

Assumptions

A schematic diagram of the physical model is illustrated in Fig. 1. A vertical semi-infinite solid fuel (region I) is exposed to external thermal radiation.

NOMENCLATURE

a_g	absorption coefficient for absorbing gases
A_p	frequency factor for pyrolysis
A_r	frequency factor for gas-phase chemical reaction
C	specific heat [$\mathrm{J\,g^{-1}\,K^{-1}}$]
C_1, C_2	constants for ignition criteria
C_i	mass fraction for species i
D	molecular diffusivity [$\mathrm{cm^2\,s^{-1}}$]
E_p	pyrolysis activation energy [$\mathrm{J\,mol^{-1}}$]
E_r	gas-phase reaction activation energy [$\mathrm{J\,mol^{-1}}$]
F	flux sum [$\mathrm{W\,cm^{-2}}$]
Gr_x	Grashof number $[g\beta_T(T_i - T_\infty)x^3]/\nu^2$
h	heat transfer coefficient [$\mathrm{W\,cm^{-2}\,K^{-1}}$]
I	intensity of radiation [$\mathrm{W\,cm^{-2}}$]
I_b	intensity of blackbody radiation [$\mathrm{W\,cm^{-2}}$]
k	thermal conductivity [$\mathrm{W\,cm^{-1}\,K^{-1}}$]
L_i	pyrolysis heat release [$\mathrm{J\,g^{-1}}$]
$\dot{m}_i'''$	generation rate of mass species i [$\mathrm{g\,cm^{-3}\,s^{-1}}$]
n	stoichiometric constant
P	total pressure
Pr	Prandtl number
$\dot{q}''$	heat flux [$\mathrm{W\,cm^{-2}}$]
Q	net radiation heat flux [$\mathrm{W\,cm^{-2}}$]
Q_H	heat of combustion [$\mathrm{J\,g^{-1}}$]
R	universal gas constant [$\mathrm{J\,K^{-1}\,mol^{-1}}$]
$\dot{S}_g'''$	energy generation rate [$\mathrm{W\,cm^{-3}}$]
t	time [s]
T	temperature [K]
T_i	ignition temperature [K]
v	velocity [$\mathrm{cm\,s^{-1}}$]
x	coordinate along the surface or height of the fuel [cm]
y	coordinate normal to the surface [cm].

Greek symbols

α	thermal diffusivity [$\mathrm{cm^2\,s^{-1}}$]
β_T	volumetric coefficient of thermal expansion [$\mathrm{K^{-1}}$]
δ	thickness of the natural-convection boundary layer [cm]
η	dimensionless coordinate normal to the surface
θ	dimensionless temperature or angle of the directional radiation
θ_p	dimensionless pyrolysis activation energy, E_p/RT
θ_r	dimensionless gas-phase reaction activation energy, E_r/RT
κ	absorption coefficient [$\mathrm{cm^{-1}}$]
μ	$\cos\theta$
ν	kinematic viscosity [$\mathrm{cm^2\,s^{-1}}$]
ρ	density [$\mathrm{g\,cm^{-3}}$]
σ	Stefan–Boltzmann constant [$\mathrm{W\,cm^{-2}\,K^{-4}}$]
τ	dimensionless time
ψ	stream function
ω_j	weight for the jth quadrature
Ω	solid angle [sr].

Subscripts

a	absorption
b	blackbody
e	effective
f	fuel
g	gas phase
I, II	regions I and II
o	external radiation source
ox	oxidizer
p	Planck mean or pyrolysis
pr	combustion products
r	chemical reaction
R	thermal radiation
s	solid phase
∞	ambient.

Superscripts

$+$	positive y-direction
$-$	negative y-direction
$\cdot$	time derivative.

Initially, the temperature of the system increases through the inert conduction of the absorbed radiant energy by the solid phase. When the surface temperature is sufficiently high, an endothermic decomposition (gasification) process begins at the surface and the surface temperature quickly ceases to rise. The pyrolyzed gases start to diffuse away from the surface and to mix with surrounding oxidizers in the gas-phase region (II). Heat release from chemical reactions in the mixed gases and radiation energy absorbed by the gas phase increase the gas-phase temperature and accelerate the exothermic gas-phase reaction. Finally a thermal runaway condition is reached and ignition occurs. During the process, a buoyant boundary layer flow is inevitably induced along the surface due to the gravitational force, enhancing the cooling of the surface, and diluting the absorbing gases. Cooling, dilution, and flushing of the gas mixture by natural-convection flows retard ignition, while radiation absorption in the gas phase shortens the ignition delay times.

The following simplifications are assumed in the formulation of the mathematical model for radiation induced ignition of solid fuels.

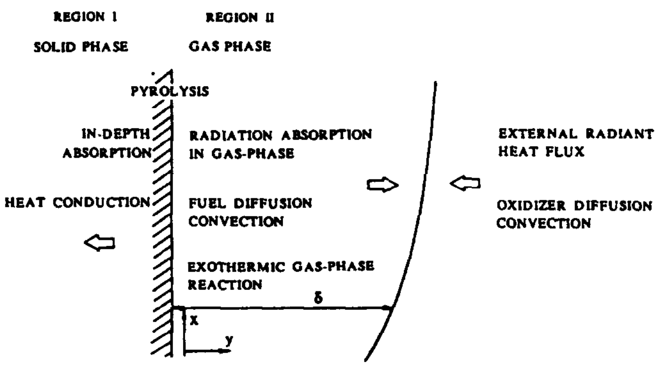

FIG. 1. Schematic of the physical model for radiation induced ignition of solid fuels

(1) The process is one-dimensional and transient.

(2) The external pressure is constant and the gas mixture behaves like a perfect gas.

(3) Thermophysical properties of the solid phase and the specific heat, $\rho_g^2 D_g$ and $\rho_g k_g$ of the gas phase are constant with respect to temperature variation.

(4) The Lewis number for the gas mixture is unity.

(5) Pyrolysis of a solid fuel occurs only at the surface and its rate is formulated by a single zero-order reaction of Arrhenius law.

(6) Gas-phase chemical reaction is modeled by a single step of the form

$$\text{Fuel} + [n]\,\text{Oxidizer} \rightarrow [n+1]\,\text{Products}$$

and a global second-order reaction of Arrhenius law.

(7) Molecular weights of all species are constant and equal.

(8) Radiation absorption coefficients of the gas mixture are proportional to the sum of the mass fractions of the pyrolyzed gases and combustion products: $\kappa_g = a_g P(C_f + C_{pr})$, where a_g represents the absorption coefficient for the absorbing gas at 1 atm partial pressure.

(9) Scattering of radiation by the decomposition particles is negligible.

(10) Effects incurred by natural convection are approximated by a thin boundary layer thickness (δ in Fig. 1) for transport phenomena and the effective conductivities (k_e) and diffusivities (D_e) of the gaseous mixture in the boundary layer.

Assumptions (1)–(7) are generally made in many combustion studies [1]. Assumption (8) is made to estimate the radiation properties of absorbing gases within a simple framework of the simulation. Assumption (9) is valid, if the volume fraction of particles generated during the ignition process is small or the size parameters for scattering are small [13]. Otherwise, scattering of radiation by particles should be considered since it reduces the radiative energy input to the fuel. For the present study, the scattering is neglected partly for the simplicity of the problem and partly due to the lack of adequate information about generated particles during the rapid ignition process. Lastly, assumption (10) is made to accommodate the natural convection effects in the one-dimensional analysis, although this approximation cannot fully describe the natural convection effects.

Formulation

Subject to the stated assumptions, the governing equations in the theoretical model for radiation induced ignition of solid fuels are given as follows:

energy conservation for solid phase (region I)

$$\rho_s C_s\left(\frac{\partial T}{\partial t} + v_p \frac{\partial T}{\partial y}\right) = \frac{\partial}{\partial y}\left(k_s \frac{\partial T}{\partial y}\right) - \frac{d\dot{q}''_R}{dy}; \qquad (1)$$

mass conservation for gas phase (region II)

$$\frac{\partial \rho_g}{\partial t} + \frac{\partial(\rho_g v)}{\partial y} = 0; \qquad (2)$$

gas-phase energy conservation

$$\rho_g C_g\left(\frac{\partial T}{\partial t} + v \frac{\partial T}{\partial y}\right) = \frac{\partial}{\partial y}\left(k_e \frac{\partial T}{\partial y}\right) + \dot{S}'''_g - \frac{d\dot{q}''_R}{dy}; \qquad (3)$$

gas species conservation

$$\rho_g\left(\frac{\partial C_i}{\partial t} + v \frac{\partial C_i}{\partial y}\right) = \frac{\partial}{\partial y}\left(\rho_g D_e \frac{\partial C_i}{\partial y}\right) + \dot{m}'''_i; \qquad (4)$$

equation of state

$$\rho_g T = \rho_{g,\infty} T_\infty. \qquad (5)$$

In the above, the subscript i represents fuel (f), oxidizer (ox), and combustion products (pr). The energy generation rate $\dot{S}'''_g$ in equation (3) and the mass reaction rate $\dot{m}'''_i$ in equation (4) are modeled as

$$\dot{m}'''_f = -\rho_g^2 C_f C_{ox} A_r e^{-E_r/RT} \qquad (6)$$

$$\dot{m}'''_f = \frac{\dot{m}'''_{ox}}{n} = -\frac{\dot{m}'''_{pr}}{n+1} = -\frac{\dot{S}'''_g}{Q_H} \qquad (7)$$

where n is the stoichiometric constant and Q_H the heat of combustion.

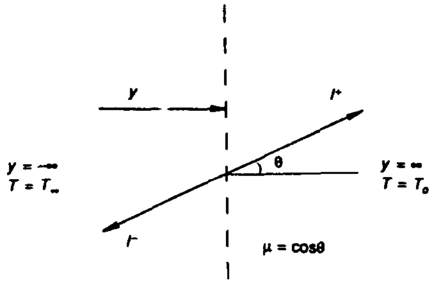

FIG. 2. Coordinate system for radiative transfer.

The equation of radiative transfer is given as

$$\mu \frac{\mathrm{d}I}{\mathrm{d}y} = \kappa I_{\mathrm{b}} - \kappa I \tag{8}$$

where I is the directional intensity of radiation and $\mu = \cos\theta$, as shown in Fig. 2. Using the directional intensity, radiation source terms in equations (1) and (3) are expressed as

$$\frac{\mathrm{d}\dot{q}''_{\mathrm{R}}}{\mathrm{d}y} = 4\kappa\sigma T^4 - \kappa \int_{4\pi} I(y, \Omega)\,\mathrm{d}\Omega. \tag{9}$$

The resulting equations must satisfy the following initial and boundary conditions:

for $t \leqslant 0$

$$T = T_\infty, \quad C_{\mathrm{f}} = C_{\mathrm{pr}} = 0, \quad C_{\mathrm{ox}} = 0.2; \tag{10}$$

for $t > 0$ and $y \to -\infty$

$$T = T_\infty, \quad I^+ = \frac{\sigma T_\infty^4}{\pi}; \tag{11}$$

for $t > 0$ and $y = 0$

$$-k_{\mathrm{e}} \frac{\partial T}{\partial y} = -k_{\mathrm{s}} \frac{\partial T}{\partial y} + \rho_{\mathrm{s}} v_{\mathrm{p}} L_i \tag{12}$$

$$-\rho_{\mathrm{g}} D_{\mathrm{e}} \frac{\partial C_{\mathrm{f}}}{\partial y} + \rho_{\mathrm{g}} v C_{\mathrm{f}} = \rho_{\mathrm{s}} v_{\mathrm{p}} \tag{13}$$

$$-\rho_{\mathrm{g}} D_{\mathrm{e}} \frac{\partial C_{\mathrm{ox}}}{\partial y} + \rho_{\mathrm{g}} v C_{\mathrm{ox}} = 0 \tag{14}$$

$$-\rho_{\mathrm{g}} D_{\mathrm{e}} \frac{\partial C_{\mathrm{pr}}}{\partial y} + \rho_{\mathrm{g}} v C_{\mathrm{pr}} = 0 \tag{15}$$

$$T_{\mathrm{I}} = T_{\mathrm{II}}, \quad v_{\mathrm{p}} = A_{\mathrm{p}} \mathrm{e}^{-E_{\mathrm{p}}/RT}; \tag{16}$$

for $t > 0$ and $y = \delta$

$$T = T_\infty, \quad C_{\mathrm{f}} = C_{\mathrm{pr}} = 0, \quad C_{\mathrm{ox}} = 0.2, \quad I^- = \frac{\sigma T_0^4}{\pi}. \tag{17}$$

Nondimensionalization and transformation

It is convenient to employ the stream function

$$\psi = \int_0^y \rho_{\mathrm{g}}\,\mathrm{d}y$$

in place of y as an independent variable to account for variable gas density. The non-dimensionalized variables are defined in the transformed coordinate system as follows:

$$\tau = \alpha_{\mathrm{s}} \kappa_{\mathrm{s}}^2 t, \quad \eta_{\mathrm{s}} = \kappa_{\mathrm{s}} y_{\mathrm{s}}, \quad \eta_{\mathrm{g}} = \frac{a_{\mathrm{g}} P_\infty}{\rho_{\mathrm{g},\infty}} \psi \tag{18}$$

$$\theta = \frac{T}{T_\infty}, \quad \theta_{\mathrm{p}} = \frac{E_{\mathrm{p}}}{RT_\infty}, \quad \theta_{\mathrm{r}} = \frac{E_{\mathrm{r}}}{RT_\infty}. \tag{19}$$

The governing equations, initial and boundary conditions are transformed to the following:

solid phase energy

$$\frac{\partial \theta}{\partial \tau} = \frac{\partial^2 \theta}{\partial \eta_{\mathrm{s}}^2} - \frac{v_{\mathrm{p}}}{\alpha_{\mathrm{s}} \kappa_{\mathrm{s}}} \frac{\partial \theta}{\partial \eta_{\mathrm{s}}} - \frac{\dfrac{\mathrm{d}\dot{q}''_{\mathrm{R}}}{\mathrm{d}y}}{\alpha_{\mathrm{s}} \kappa_{\mathrm{s}}^2 \rho_{\mathrm{s}} C_{\mathrm{s}} T_\infty}; \tag{20}$$

gas phase energy

$$\frac{\partial \theta}{\partial \tau} = \frac{\alpha_{\mathrm{g},\infty}}{\alpha_{\mathrm{s}}} \left(\frac{a_{\mathrm{g}} P_\infty}{\kappa_{\mathrm{s}}}\right)^2 \frac{\partial^2 \theta}{\partial \eta_{\mathrm{g}}^2} + \frac{\left(\dot{S}'''_{\mathrm{g}} - \dfrac{\mathrm{d}\dot{q}''_{\mathrm{R}}}{\mathrm{d}y}\right)\theta}{\alpha_{\mathrm{s}} \kappa_{\mathrm{s}}^2 \rho_{\mathrm{g},\infty} C_{\mathrm{g},\infty} T_\infty}; \tag{21}$$

gas species

$$\frac{\partial C_i}{\partial \tau} = \frac{\alpha_{\mathrm{g},\infty}}{\alpha_{\mathrm{s}}} \left(\frac{a_{\mathrm{g}} P_\infty}{\kappa_{\mathrm{s}}}\right)^2 \frac{\partial^2 C_i}{\partial \eta_{\mathrm{g}}^2} - \frac{\dot{m}_i''' \theta}{\alpha_{\mathrm{s}} \kappa_{\mathrm{s}}^2 \rho_{\mathrm{g},\infty}}; \tag{22}$$

for $\tau \leqslant 0$

$$\theta = 1, \quad C_{\mathrm{f}} = C_{\mathrm{pr}} = 0, \quad C_{\mathrm{ox}} = 0.2; \tag{23}$$

for $\tau > 0$ and $\eta_{\mathrm{s}} \to -\infty$

$$\theta = 1; \tag{24}$$

for $\tau > 0$ and $\eta_{\mathrm{g}} = \eta_{\mathrm{s}} = 0$

$$\frac{\partial \theta}{\partial \eta_{\mathrm{g}}} = \frac{\kappa_{\mathrm{s}}}{a_{\mathrm{g}} P_\infty} \frac{k_{\mathrm{s}}}{k_{\mathrm{e},\infty}} \frac{\partial \theta}{\partial \eta_{\mathrm{s}}} - \frac{\rho_{\mathrm{s}} v_{\mathrm{p}} L_i}{a_{\mathrm{g}} P_\infty k_{\mathrm{e},\infty} T_\infty} \tag{25}$$

$$\frac{\partial C_{\mathrm{f}}}{\partial \eta_{\mathrm{g}}} - \frac{\rho_{\mathrm{s}} v_{\mathrm{p}}}{a_{\mathrm{g}} P_\infty \rho_{\mathrm{g},\infty} \alpha_{\mathrm{g},\infty}} (C_{\mathrm{f}} - 1) = 0 \tag{26}$$

$$\frac{\partial C_{\mathrm{ox}}}{\partial \eta_{\mathrm{g}}} - \frac{\rho_{\mathrm{s}} v_{\mathrm{p}}}{a_{\mathrm{g}} P_\infty \rho_{\mathrm{g},\infty} \alpha_{\mathrm{g},\infty}} C_{\mathrm{ox}} = 0 \tag{27}$$

$$\frac{\partial C_{\mathrm{pr}}}{\partial \eta_{\mathrm{g}}} - \frac{\rho_{\mathrm{s}} v_{\mathrm{p}}}{a_{\mathrm{g}} P_\infty \rho_{\mathrm{g},\infty} \alpha_{\mathrm{g},\infty}} C_{\mathrm{pr}} = 0 \tag{28}$$

$$\theta_{\mathrm{I}} = \theta_{\mathrm{II}}, \quad v_{\mathrm{p}} = A_{\mathrm{p}} \mathrm{e}^{-\theta_{\mathrm{r}}/\theta}; \tag{29}$$

for $\tau > 0$ and $\eta_{\mathrm{g}} = a_{\mathrm{g}} P_\infty \psi(\delta)/\rho_{\mathrm{g},\infty}$

$$\theta = 1, \quad C_{\mathrm{f}} = C_{\mathrm{pr}} = 0, \quad C_{\mathrm{ox}} = 0.2. \tag{30}$$

The directional intensity of radiation within the medium, $I(y, \theta)$, can be divided into two contributions: the intensity directed in the positive y-direction, denoted by I^+, and that directed in the negative direction, denoted by I^- as illustrated in Fig. 2. Thus, equation (8) can be decomposed as in the positive y-direction

$$\mu \frac{dI^+}{dy} = \kappa I_b - \kappa I^+ \tag{31}$$

and in the negative direction

$$-\mu \frac{dI^-}{dy} = \kappa I_b - \kappa I^-. \tag{32}$$

As in the flux model [14], a net radiation heat flux Q is defined as

$$Q = I^+ - I^- \tag{33}$$

and a flux sum F as

$$F = \frac{I^+ + I^-}{2}. \tag{34}$$

Equations (31) and (32) can be replaced by the following equations in terms of Q and F:

$$-\mu^2 \frac{d}{dy}\left(\frac{1}{\kappa}\frac{dF}{dy}\right) = \kappa I_b - \kappa F \tag{35}$$

$$Q = -\frac{2\mu}{\kappa}\frac{dF}{dy} \tag{36}$$

and equation (9) can be rewritten as

$$\frac{d\dot{q}''_R}{dy} = 4\kappa\sigma T^4 - 4\pi\kappa \int_0^1 F\, d\mu. \tag{37}$$

The integration in the second term of the right-hand side of equation (37) can be approximated by the sum of the finite number of discrete Gaussian quadratures [15] as

$$\frac{d\dot{q}''_R}{dy} = 4\kappa\sigma T^4 - 4\pi\kappa \sum_{j=1}^{M} F_j \omega_j. \tag{38}$$

For the present study the space of the system is divided into ten quadratures ($M = 5$). The relevant boundary conditions for equation (38) are given as, at $y = -\infty$

$$F_j + \frac{Q_j}{2} = F_j - \frac{\mu_j}{\kappa}\frac{dF_j}{dy} = \frac{\sigma T_\infty^4}{\pi} \tag{39}$$

and at $y = \delta$

$$F_j - \frac{Q_j}{2} = F_j + \frac{\mu_j}{\kappa}\frac{dF_j}{dy} = \frac{\sigma T_o^4}{\pi}. \tag{40}$$

As the governing equations describing the ignition phenomena are highly nonlinear and coupled in a complex manner, they were solved numerically using the Crank–Nicholsen scheme. Appropriate tests on stability and convergence were successfully satisfied. Table 1 shows the physical and chemical constants used for the study on radiation induced ignition. Since detailed information about the gas phase is not available during the rapid ignition process, the properties of air at 300 K are used for those of the gas phase, except for the absorption coefficient (a_g). The absorption coefficient (a_g) for the gas phase varies from 0 to 10 atm^{-1} cm^{-1} in the present analysis because the Planck mean absorption coefficient for a typical plastic gas (MMA vapor) is about 1 atm^{-1} cm^{-1} at the gas-phase temperatures below 800 K [16]. The properties of the solid phase are typical values of plastic materials [1].

Table 1. Physical and chemical properties used in this study

A_p [cm s^{-1}]	5.5×10^8
A_r [cm^3 g^{-1} s^{-1}]	10^9
$C_{g,\infty}$ [J g^{-1} K^{-1}]	1.005
C_s [J g^{-1} K^{-1}]	1.42
$k_{g,\infty}$ [W cm^{-1} K^{-1}]	2.61×10^{-4}
k_s [W cm^{-1} K^{-1}]	1.9×10^{-3}
L_r [J g^{-1}]	−1250
n	8
P_∞ [atm]	1
Q_H [J g^{-1}]	26 120
T_o [K]	1400
x [cm]	10
$\alpha_{g,\infty}$ [cm^2 s^{-1}]	0.2216
α_s [cm^2 s^{-1}]	1.12×10^{-3}
θ_p	66.7
θ_r	30
κ_s [cm^{-1}]	100

RESULTS AND DISCUSSION

The present study emphasizes effects of gas-phase radiation absorption on the radiative ignition of solid fuels. Evidence that pyrolyzed gases absorb a significant amount of external radiation energy can be found through the transmittance of the incident radiation at the fuel surface. Transmittances of the incident radiation through the pyrolyzed gases during the ignition process predicted for the zero gravity case and for a vertical surface with gravity effects are shown in Fig. 3. The theoretical transmittances for three different radiation sources are compared with the experimental results obtained by Kashiwagi [9] in this figure. In general, experimental results (dotted lines) are bounded by the two theoretical transmission curves (solid and dashed lines) at large times. Under zero gravity conditions, pyrolyzed fuel gases accumulate near the solid-fuel surface and diffuse normal to the surface, so that all absorbing gases participate in

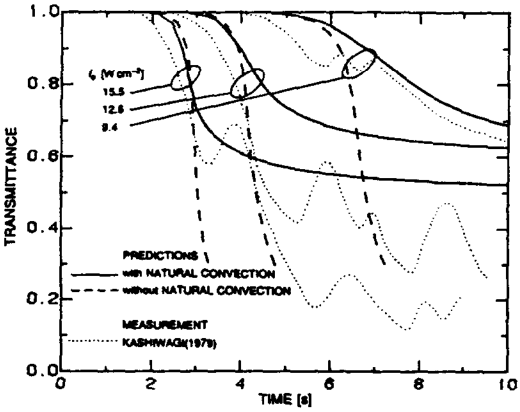

FIG. 3. Transmittance of incident radiation through the gas phase with absorption coefficient $a_g = 1.9$ atm^{-1} cm^{-1}.

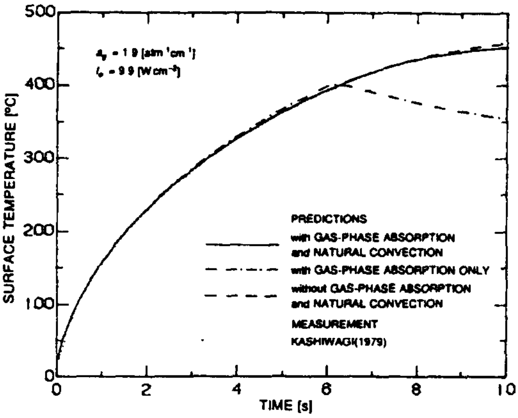

FIG. 4 Comparison of surface temperature rise

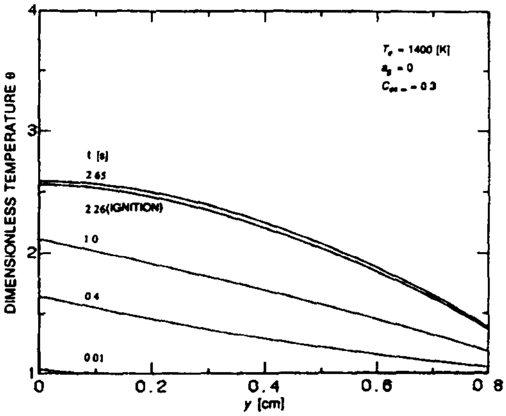

FIG. 5. Temperature profile histories for the gas-phase region without gas-phase radiation absorption.

the radiation energy exchange. On the other hand, for a vertical surface under gravity the pyrolyzed gases from the fuel cannot accumulate near the surface due to the dilution and flushing by the natural-convection flows. Since the experiment [9] was conducted on horizontally positioned solid fuels under the gravitational condition with the incident radiation directing downwards, a plume was induced over the surface and the decomposed gases were diluted and cooled by the plume motion and air entrainment. The plume, however, attenuates the incident radiation more than the natural convection boundary layer flow along a vertical surface since the direction of the flow in the plume is almost parallel to the line of sight of the external radiation, the laser beam in this case. The wandering motion and air entrainment in the plume for a horizontally positioned fuel dilute the pyrolyzed gases and cause the fluctuations visible in the experimental curves, resulting in less attenuation of the incident radiation than that for the zero gravity case. Since a 10.6 μm wavelength CO_2 laser was used as a radiation source in Kashiwagi's experiment, the estimated absorption coefficient ($a_g = 1.9$ atm^{-1} cm^{-1}) of MMA vapor [16] at that wavelength was used in the predictions presented in Figs. 3 and 4. Figure 4 compares predicted surface temperature rises to the experimental data. During the initial inert-heating stage (which is up to 6 s), differences between theoretical and experimental results are not yet significant. Soon after, however, the pyrolysis reaction becomes active and the pyrolyzed gases begin to block the incident radiation. Due to active endothermic pyrolysis reactions and radiation blockage the surface temperature ceases to rise. This trend can be seen in the experimental measurements (dotted line). While the comparison of the dash-dot line with the dotted line shows that the zero gravity effect results in an exaggerated radiation blockage, comparison of the solid line with the dotted line indicates that the incident radiation for the vertical fuel is attenuated less than for the horizontal fuel as was indicated in Fig. 3.

At the present development stage of the ignition theory, the exact state of theoretical ignition is itself a poorly defined concept, while the experimental measurement of ignition delay time is based on the detection of the emission of light. Although there are many theoretical ignition criteria, the ignition delay time is not sensitive to any particular ignition criterion [1]. For gas-phase ignition, only the following criteria would describe the process mechanistically [6]: (1) critical local gas temperature increase rate ($\partial T/\partial t \geqslant C_1$); (2) gas temperature gradient reversal at the solid–gas interface ($(\partial T/\partial y)_{y=0} = 0$); and (3) critical total reaction rate in the boundary layer

$$\left(\int_0^{\delta} \dot{m}_{\mathrm{f}}''' \,\mathrm{d}y \geqslant C_2\right).$$

Thermal criteria (1) and (2) cannot predict ignition delay times properly because radiation energy absorbed in the gas phase can increase the gas-phase temperature to satisfy the thermal criteria without any help from gas-phase chemical reactions. A runaway condition is, however, ultimately reached through chemical reactions. Therefore, the ignition criteria need to be related to the chemical reaction process. For the present analysis, the third criterion has been selected with $C_2 = 2 \times 10^{-5}$ [g cm^{-2} s^{-1}] [1].

Figures 5 and 6 present dimensionless temperature

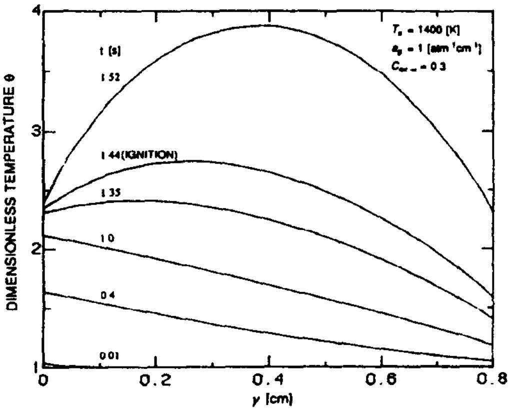

FIG. 6. Temperature profile histories for the gas-phase region with gas-phase radiation absorption.

profiles in the gas phase at various times without and with considerations of radiation absorption in the gas phase, respectively. According to the previously defined ignition criterion, ignition for absorbing gases occurs much earlier than that for the non-absorbing gases. After the onset of ignition, temperature profiles from two theoretical predictions show totally different trends. For the non-absorbing gases shown in Fig. 5, the temperature gradient at the fuel surface, which is almost zero, indicates that chemical reaction in the gas phase barely manages to generate the thermal energy to compensate for the heat loss to the surroundings and is not sufficiently active to increase the gas-phase temperature significantly as in a real fire situation. In this case, the ignition process seems to be governed by near-surface chemical reaction or heat conduction from the solid phase. For the absorbing gases, however, there is a sudden increase in the gas-phase temperature just after the ignition, as shown in Fig. 6, which realistically simulates an ignition phenomenon.

Time histories of the radiant energy emitted from the system to the surroundings calculated at $y = 0$ and δ using the same conditions that were used in Fig. 6 are shown in Fig. 7. The difference between the two curves at each time represents the radiation energy emitted purely from the gas phase. Until the theoretical ignition point ($t = 1.44$ s), the radiation energy emitted from the gas phase is negligible due to the low gas-phase temperature and the low concentration of the absorbing gases. Just after the ignition, however, an abrupt jump of the radiation energy emitted from the gas phase is predicted. Thus, the separation of the solid line from the dashed line can be used as another theoretical ignition point, which is similar to the experimental definition of ignition, although it is not related with chemical reaction.

To understand the mechanism of radiation induced ignition, a comparison between heat release from gas-phase chemical reaction and absorbed radiation energy in the gas phase is made at the moment of temperature reversal at the fuel surface.

Heat release from chemical reactions is

$$Q_H \rho^2 C_f C_{ox} A_r e^{-\theta_r/\theta}$$

$$= 26\,120\left(\frac{0.00118}{2.3}\right)^2 C_f 0.2 \times 10^9 e^{-30/2.3} = 2.96 C_f \tag{41}$$

where the surface temperature, θ, at reversal is about 2.3, as shown in Fig. 6.

Radiation energy absorbed is

$$-\frac{dq_R''}{dy} = -4\kappa_g \sigma T^4 + \kappa_g \int_{4\pi} I(y,\Omega)\, d\Omega$$

$$\approx -4a_g P_\infty C_f(\sigma T^4 - 0.5\sigma T_o^4)$$

$$= 5.89 C_f \quad \text{for } T_o = 1000 \text{ K}$$

$$= 51.96 C_f \quad \text{for } T_o = 1500 \text{ K} \tag{42}$$

using typical values for the fuel properties (see Table 1) and 1 atm^{-1} cm^{-1} for a_g. When the source temperature is 1000 K, the heat release from chemical reaction is comparable to the energy absorbed by pyrolyzed gases. As the strength of external radiation source increases, the radiation absorption is proven to be a much stronger source during energy transport than chemical heat release. Hence, it can be deduced that the runaway condition is strongly dependent on both the radiation absorption of pyrolyzed gases and heat release from chemical reactions during the ignition process for intense radiation sources.

Figure 8 shows ignition delay times as a function of the initial oxygen mass fractions. For the initial oxygen concentration larger than 0.3, the differences between the predicted results are not significantly large. But for lower concentrations, the differences are significant. It appears that while ignition may not occur for non-absorbing gases under the normal atmospheric condition, it can be achieved for absorbing gases under lower oxygen concentration conditions. Since the oxygen concentration in a real fire accident is smaller than in the normal situation ($C_{ox,\infty} = 0.2$), gaseous radiation absorption effects

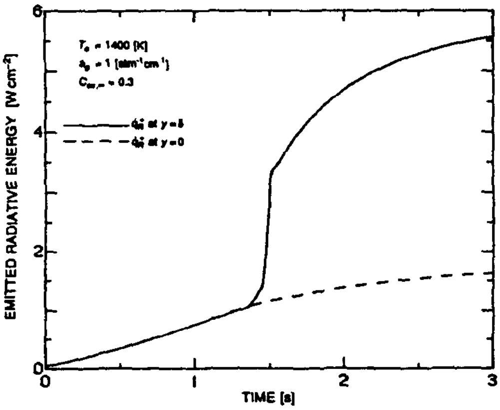

FIG. 7. Radiative energy emitted from the fuel.

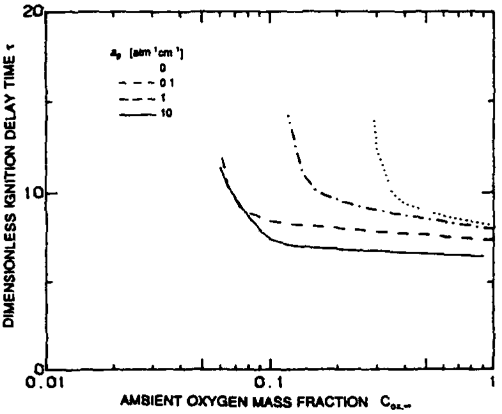

FIG. 8. Effect of the ambient oxygen mass fraction on ignition delay times.

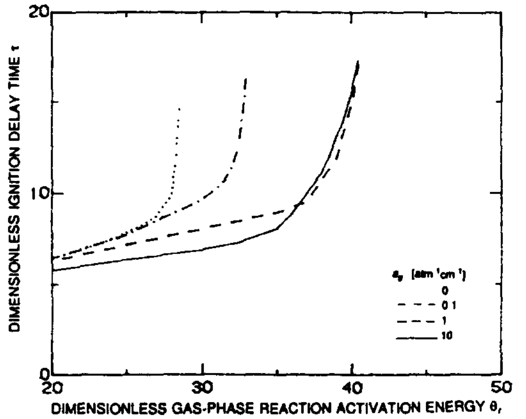

FIG. 9. Effect of gas-phase reaction activation energy on ignition delay times.

should be considered for more realistic predictions of the radiative ignition phenomena.

To investigate the effects of the chemical parameters on the ignitable domain, the ignition delay time is calculated and presented for the variations of the gas-phase reaction activation energy and of the pyrolysis activation energy in Figs. 9 and 10, respectively. Figure 9 shows that only an upper limit of the gas-phase reaction activation energy exists for all gases. This is in contrast to the studies for non-absorbing gases at zero gravity by Kashiwagi [1], in which both upper and lower limits are predicted. Under the zero gravity condition and for low values of the reaction activation energy, chemical reactions during the initial stage are not active due to the low gas-phase temperature and the lack of sufficient fuel gases. Oxidizers are, however, consumed fairly rapidly owing to the high value of the stoichiometric constant and the low values of the reaction activation energy. During the later stage, sufficient oxidizer is not available, although sufficient fuel gases are available. The lack of fuel supply during the initial stage and the exhaustion of oxidizers at the later stage of the process prevent ignition from occurring. Such depletion of oxidizers, however, does not occur in the practical situations, because natural convection flows enhance the mixing of the fuel gases with the ambient oxidizers and supply the ambient oxidizers continuously to the fuel gases inside the thin boundary layer. In Fig. 10, the ignition delay times for all gases are not significantly different for dimensionless pyrolysis activation energies θ_p larger than 80. For such high pyrolysis activation energies, the fuel is not pyrolyzed at low surface temperatures. When the surface temperature becomes high enough to assist an active pyrolysis reaction, the gas-phase temperature is already high enough to boost chemical reactions. Thus, ignition is governed by chemical reaction with gas-phase radiation absorption assisting in chemical reactions as well. For activation energies lower than 70, ignition is mainly governed by gas-phase radiation absorption. In this region, the θ_p is so low that pyrolysis of a solid fuel starts at low surface temperature. Fuel species are then rapidly accumulated near the surface. The concentrations of fuel and oxygen species are rich enough to react chemically during the initial stage, but the gas phase is not hot enough to accelerate the gas-phase reaction. With increasing time, a large amount of fuel species displays oxygen away from the surface, but the natural convection flow continuously supplies oxidizers inside the boundary layer. Thus, the region in which mixture of sufficient fuel and oxidizer species is available is formed further away from the surface than that for the higher activation energy case. If the pyrolyzed gases are not infrared active, the temperature in this region is not sufficiently high to support chemical reaction due to the relatively high value of the gas-phase chemical reaction activation energy, meaning that ignition cannot occur. For absorbing gases, however, some portion of the incident radiation energy is absorbed and transformed in the internal energy of the gases. As a result, the absorbed energy increases the gas-phase temperature to activate gas-phase chemical reaction, until ultimately, ignition is achieved.

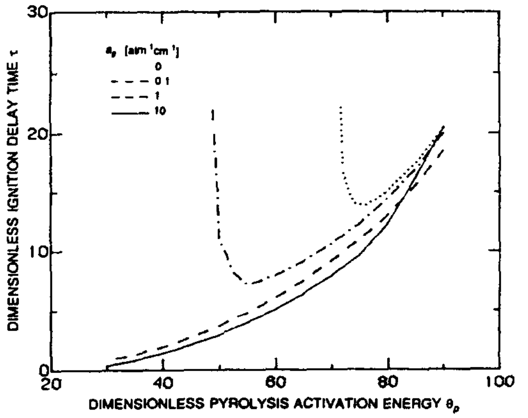

FIG. 10. Effect of pyrolysis activation energy on ignition delay times.

CONCLUSIONS

A comprehensive analysis of radiation induced ignition of solid fuels has been carried out. Effects of the absorption of incident radiation by the gas phase and the natural convection along the vertical fuel surface are included in the analysis. Absorbed radiation energy is calculated in the radiation flux-type transfer equation. Natural convection effects are approximated through the thin gas-phase boundary layer and effective conductivities in the layer.

Transmittance curves of the incident radiation calculated at the fuel surface indicate that a significant amount of the incident radiation is attenuated in the gas-phase region, even for the case of vertical surfaces under the normal gravitational condition. The slow increase of the surface temperature at the later stage of the ignition process is attributed to both the radiation blockage by the pyrolyzed gases and cooling mechanisms such as natural convection, endothermic pyrolysis, and radiation emission.

A theoretical ignition point almost coincides with the abrupt increase of the radiation emission from the gas-phase region. Ignition delay times for highly absorbing gases are not sensitive to the variation of the absorption coefficient of the participating gases. Lower limits in the value of the gas-phase reaction activation energy for ignition are not predicted, which is due to the continuous supply of the ambient oxidizer to the gas-phase region by the natural-convection flows along the surface and relatively low values of the reaction activation energy. While lower limits in the value of the pyrolysis activation energy still exist for weakly absorbing gases, they do not appear for the intermediate or highly absorbing gases owing to the radiation absorption by the gas phase. Under less favorable physical and chemical conditions to achieve ignition, ignition is mainly governed by gas-phase radiation absorption.

Acknowledgement—The authors wish to express their appreciation to the National Institute of Standards and Technology, Center for Fire Research for their support of this research.

REFERENCES

1. T. Kashiwagi, A radiative ignition model of a solid fuel, *Combust. Sci. Technol.* **8,** 225–236 (1974).
2. M. Kindelan and F. A. Williams, Theory for endothermic gasification of a solid by a constant energy flux, *Combust. Sci. Technol.* **10,** 1–9 (1975).
3. M. Kindelan and F. A. Williams, Radiant ignition of a combustible solid with a gas-phase exothermicity, *Acta Astronautica* **2,** 955–976 (1976).
4. M. Kindelan and F. A. Williams, Gas-phase ignition of a solid with in-depth absorption of radiation, *Combust. Sci. Technol.* **16,** 47–58 (1977).
5. R. K. Kumar, Gas phase ignition of a composite solid propellant subjected to radiant heating, *Combust. Sci. Technol.* **30,** 273–288 (1983).
6. P. D. Gandi and A. M. Kanury, Criterion for spontaneous ignition of radiantly heated organic solids, *Combust. Sci. Technol.* **50,** 233–254 (1986).
7. N. Mutoh, T. Hirano and K. Akita, Experimental study on radiative ignition of polymethylmethacrylate, *Seventeenth Symp. (Int.) on Combustion*, pp. 1183–1190. The Combustion Institute, Pittsburgh, Pennsylvania (1978).
8. T. Kashiwagi, Experimental observation of radiative ignition mechanisms, *Combust. Flame* **34,** 231–244 (1979).
9. T. Kashiwagi, Effects of attenuation of radiation on surface temperature for radiative ignition, *Combust. Sci. Technol.* **20,** 225–234 (1979).
10. B. Amos and A. C. Fernandez-Pello, Model of the ignition and flame development on a vaporizing combustible surface in a stagnation point flow: ignition by vapor fuel radiation absorption, *Combust. Sci. Technol.* **62,** 331–343 (1988).
11. B. Amos, H. Kodama and A. C. Fernandez-Pello, An analysis of the ignition and flame propagation caused by vapor radiation absorption of a vaporing fuel at zero gravity, *Prog. Astronaut. Aeronaut.* (to appear).
12. D. Drysdale, *An Introduction to Fire Dynamics.* Wiley, New York (1985).
13. H. C. Van de Hulst, *Light Scattering by Small Particles.* Wiley, New York (1957).
14. A. D. Gosman and F. C. Lockwood, Incorporation of a flux model for radiation into a finite-difference procedure for furnace calculations, *Fourteenth Symp. (Int.) on Combustion*, pp. 661–671. The Combustion Institute, Pittsburgh, Pennsylvania (1975).
15. S. Kumar, A. Majumdar and C. L. Tien, The differential-discrete-ordinate method for solving the general equation of radiative transfer, *Proc. ASME AIChE 25th National Heat Transfer Conf.* (Houston), Vol. 1, pp. 178–185 (1988). Also, to appear in *J. Heat Transfer.*
16. S. H. Park, A. J. Stretton and C. L. Tien, Infrared radiation properties of methyl methacrylate vapor, *Combust. Sci. Technol.* **62,** 257–271 (1988).

INFLAMMATION DE COMBUSTIBLES SOLIDES INDUITE PAR RAYONNEMENT

Résumé—On montre que l'absorption du rayonnement par la phase gazeuse est l'un des mécanismes critiques responsables de l'allumage de la phase gazeuse des combustibles solides qui sont exposés à un rayonnement thermique externe intense. Un modèle monodimensionnnel inclut les effets de l'absorption par la phase gazeuse du rayonnement thermique incident, de l'absorption par la phase solide et de la convection naturelle autour de la surface du combustible. Une simulation numerique confirme que les produits de décomposition atténuent le rayonnement incident comme observé expérimentalement. Malgré les écoulements de convection naturelle qui diluent les gaz absorbants et augmentent les pertes thermiques, l'énergie radiative absorbée joue un rôle important dans l'induction du comportement thermique de la phase gazeuse. Ainsi les domaines d'inflammation sont considérablement différents de ceux obtenus sans tenir compte de l'absorption radiative de la phase gazeuse.

STRAHLUNGSINDUZIERTE ZÜNDUNG FESTER BRENNSTOFFE

Zusammenfassung—Es wird dargelegt, daß die Strahlungsabsorption in der Gasphase einer der kritischen Mechanismen für die Zündung fester Brennstoffe in einer Gasphase bei starker äußerer Wärmestrahlung ist. Es wird ein eindimensionales instationäres Modell verwendet, das folgende Einflüsse berücksichtigt: die Absorption einer einfallenden äußeren Wärmestrahlung in der Gasphase, die Absorption der Strahlung im Festkörper und die natürliche Konvektion an der Oberfläche des Brennstoffs. Die Ergebnisse einer numerischen Simulation bestätigen, daß die Zerfallsprodukte die einfallende Strahlung merklich schwächen—dies war bereits früher experimentell beobachtet worden. Trotz der natürlichen Konvektionsströmung, welche die absorbierenden Gase verdünnt und die Wärmeverluste erhöht, spielt die absorbierte Strahlungsenergie eine wichtige Rolle bei der Auslösung der thermischen Kettenreaktion. Somit unterscheiden sich die zündfähigen Gebiete erheblich von denen, welche ohne Betrachtung der Absorption der Gasphase erhalten werden.

ИНДУЦИРОВАННОЕ ИЗЛУЧЕНИЕМ ВОСПЛАМЕНЕНИЕ ТВЕРДЫХ ТОПЛИВ

Аннотация—Поглощение излучения газовой фазой является одним из критических механизмов, обусловливающих газофазное воспламенение твердых топлив, подверженных действию сильного внешнего теплового изучения. Одномерная нестационарная модель учитывает эффекты поглощения газовой фазой падающего теплового излучения, поглощения в объеме твердой фазы, а также естественной конвекции у поверхности топлива. Численное моделирование подтверждает экспериментально наблюдавшееся ослабление падающего излучения продуктами распада. Несмотря на то, что течения при естественной конвекции разбавляют поглощающие газы и увеличивают тепловые потери, поглощаемая энергия излучения играет важную роль индукции теплоотдачи газовой фазы. Таким образом, воспламеняющиеся области значительно отличаются от полученных без учета поглощения излучения газовой фазой.